Sensors & Actuators: B. Chemical 316 (2020) 127835

Contents lists available at ScienceDirect

Sensors and Actuators B: Chemical

journal homepage: www.elsevier.com/locate/snb

Flexible parylene-thread bioprobe and the sewing method for *in vivo* neuronal recordings

Koji Yamashita[a], Hirohito Sawahata[b], Shota Yamagiwa[a], Yusuke Morikawa[a], Rika Numano[c,d], Kowa Koida[c,e], Takeshi Kawano[a,*]

[a] Department of Electrical and Electronic Information Engineering, Toyohashi University of Technology, 1-1 Hibarigaoka Tempaku-cho, Toyohashi, Aichi 441-8580, Japan
[b] National Institute of Technology, Ibaraki College, 866 Nakane, Hitachinaka, 312-8508, Japan
[c] Electronics-Interdisciplinary Research Institute (EIIRIS), Toyohashi University of Technology, 1-1 Hibarigaoka Tempaku-cho, Toyohashi, Aichi 441-8580, Japan
[d] Department of Applied Chemistry and Life Science, Toyohashi University of Technology, 1-1 Hibarigaoka Tempaku-cho, Toyohashi, 441-8580 Japan
[e] Department of Computer Science and Engineering, Toyohashi University of Technology, 1-1 Hibarigaoka Tempaku-cho, Toyohashi 441-8580, Japan

ARTICLE INFO

Keywords:
Microelectrode
Flexible device
Neural recording
Muscle
Brain

ABSTRACT

Multichannel recording of the electrical signals from soft biological tissue of brain is an important technique in electrophysiology. However, penetration of conventional rigid needle-electrodes causes physical-stress to the tissue and induces the tissue damage, making the stable recording impossible. The approach reported here involves the use of a flexible "thread-like" device with microelectrodes that enables precise penetration and placement inside the brain tissue, with the help of a guiding microneedle, similar to sewing mechanism. A device-holding protocol, which uses a dissolvable material, is proposed to enable a stress-free "catch" and "release" of the needle. The device is placed in the primary visual cortex (V1) of an *in vivo* mouse and both the local field potentials (LFP) and the action potentials (spike) are recorded. For over a period of two weeks after device implantation, no remarkable decrease in mouse's weight is observed. Therefore, we conclude that the proposed sewing thread-device enhances the recording of neuronal signals while minimizing the device–induced stress.

1. Introduction

Recent advances in micro/nano-scale electrode device for multi-channel recording of biological signals from the tissue and the organs, such as brain, nerves, heart, and muscles play an important role in electrophysiology. However, conventional methods that use invasive rigid needle microelectrodes (e.g., 50 μm diameter or width of silicon needle) cause motion-induced stress and damage to the tissue, thereby making robust recording difficult [1–3]. In particular, for chronic applications to brain tissues, the stress at the device interface induces sustained inflammation and tissue response that will cause vascular injuries, which will ultimately result in the formation of glia and the degradation of neuron around the microelectrode site [4–6]. These chronic degradations increase the electrical interfacial impedance between the microelectrode site and neurons, increasing the noise level of the device and decreasing the signal amplitude as well as the signal to noise ratio [7,8].

The flexibility of the needle reduces penetration-induced tissue damage [2,9–11]. Furthermore, the miniaturization of the overall needle geometry (diameter or width) decreases the degree of tissue inflammation. To combine these features, micro-electro-mechanical system (MEMS) devices based on flexible materials were fabricated. However, their application was challenging as they were to be inserted into biological tissue. Furthermore, the precise penetration of the needle as well as the microelectrodes in it with respect to their position is an important consideration in electrophysiology. Moreover, these positions of microelectrode should be fixed for a long period recording (e.g., chronic device implantation). Several techniques have been proposed to penetrate the flexible needle [12–15]; however, as the next step, the penetration method requires features of minimized tissue damage and the precise position control of the microelectrodes during the penetration and fixation of these electrodes towards the chronic recording.

The approach reported in this study is based on conventional sewing mechanism. It involves the use of a "thread-like" flexible device with microelectrodes that enables precise penetration and placement inside the brain and other biological tissues with the help of a guiding microneedle. We use a tungsten microneedle, which is connected to the tip

* Corresponding author.
E-mail address: kawano@ee.tut.ac.jp (T. Kawano).

https://doi.org/10.1016/j.snb.2020.127835
Received 11 November 2019; Received in revised form 4 February 2020; Accepted 5 February 2020
Available online 06 February 2020
0925-4005/

of the flexible thread-device. Similar to conventional sewing, the tungsten microneedle plays a role during tissue penetration and guides the flexible device into the tissue; however, the tungsten needle is further entirely extracted from the tissue. To minimize physical stress to the brain tissue during device penetration, we also propose a sewing method wherein the flexible thread-bioprobe is manipulated via a dissolvable material. During the device penetration, the proposed methodology offers advantages of i) minimized tissue damage ii) precise positioning of the microelectrodes by guiding the tungsten needle, and iii) implantation capability by fixing each side of the thread's portion to the cranium.

2. Materials and methods

The proposed parylene-thread bioprobe device was fabricated based on a parylene-film MEMS process (Fig. 1a1) [16–18]. The device process was initiated with a 5-μm thick parylene film on a Si substrate. To form 5-μm-thick parylene film on a Si substrate, we used vacuum deposition equipment (model PDS2010, LABCOTER), in which an amount of parylene dimer of 9.0 g was vaporized at 175 °C, decomposed to its monomer at 690 °C, and then deposited on the Si substrate (Fig. 1a1-1). Thickness of parylene film was measured with a spectroscopic film-thickness measurement system (VM-1230, SCREEN). For both the microelectrode site and the device interconnection, a platinum (Pt, 60-nm thick) layer with an adhesion layer of titanium (Ti, 40 nm thick) was formed on the parylene film via sputtering. The formed Pt/Ti were then patented via reactive ion etching (RIE) (chamber pressure = 4.0 Pa and Ar flow rate = 20 sccm for Pt layer, and chamber pressure = 100 Pa and CF_4 flow rate = 40 sccm for Ti layer) with a photoresist (Fig. 1a1 (1,2)). The Pt/Ti layer was subsequently covered using another parylene layer (5 μm) via the same deposition parameters. For patterning the parylene layers, we used a Ti hard mask (60-nm thick), which was patterned by sputtering and etching with the same process used on the adhesion layer during device metallization (Fig. 1a1-4). The parylene layer with the Ti mask was patterned by oxygen (O_2) plasma (RIE, chamber pressure = 50 Pa, O_2 flow rate = 40 sccm). The Ti hard mask was etched away via RIE after the parylene etching (Fig. 1a1-5). Finally, the parylene film was released from the substrate using ethanol. Using this fabrication technology, we designed the 15,000 μm length and 150 μm width thread portion, which had an array of three Pt microelectrodes (10 μm × 40 μm) with a spacing of 500 μm. The overall device geometry of parylene was 33,000 μm in length, including the three pads of Pt-electrode for the external connections (Fig. S1).

Fig. 1a2 depicts the thread portion of the fabricated flexible thread-bioprobe device of parylene with a thickness of 10 μm. Each size of the fabricated Pt-electrodes shows ~15 μm × 40 μm (Fig. 1a-3, 1a-4), which are larger than the designed values (10 μm × 40 μm). This size difference is due to the over-etching of the top parylene layer (5 μm) in O_2 plasma etching (Fig. 1a1-5). The process can be improved by compensating the exceeded parylene etching. Fig. 1b depicts the packaging device in which the tip portion of the thread-bioprobe is connected to an tungsten microneedle [two types of diameters used: 150 μm (Fig. 1b) and 50 μm in animal experiment] by a ultraviolet (UV)-curable acrylic ester resin with the geometry of < 150 μm in width (Fig. S2). On the other device-sided each microelectrode's pad is connected to conventional pin connectors (three channels).

The Pt-microelectrode's impedance characteristics at 10 Hz – 10 kHz, measured in phosphate buffered saline (PBS) at room temperature, ranged from 69 ± 16 kΩ to 12 ± 3 MΩ [500 ± 100 kΩ (mean ± SD) at 1 kHz]. These were further reduced to 19 ± 2 kΩ – 1 ± 0.2 MΩ [54 ± 6 kΩ (mean ± SD) at 1 kHz] by additional plating with a low impedance material of platinum black (Pt black) [19–21] (Fig. 1c). These values are sufficiently low for measuring the neuronal activity [20–22]. As the actual sewing of the device into the tissue, a device characterization of twist test was also conducted while the electrode impedance was measured. Herein, the parylene-thread was twisted in five turns, showing no significant change in the electrode's impedance (Fig. S3).

We also explored the amplitude attenuation of recorded neuronal signals associated with the electrodes' impedance characteristics and a recording system with a preamplifier (ZC64, Tucker-Davis Technologies, USA, input resistance = 1×10^{14} Ω), as measuring the output/input signal amplitude ratios of the thread-bioprobe device with the recording system (Fig. 1d). By applying test signals of 300 μV peak-to-peak sinusoidal waves at 1 Hz – 10 kHz, the measured output/input ratios ranged from 69 % to 89 % (averages of 3 electrodes) (84 % at 1 kHz for spike recording), while the measured root mean square noise voltage was 26.4 μVrms. Considering the used test signals (300 μV, 1 kHz), the calculated signal-to-noise ratio of the recording system was 18 dB.

3. Results

Fig. 2 shows the sewing and signal recording capabilities of the fabricated thread-bioprobe device using hindlimb muscle of the mouse. The mouse (male, 20–25 g) was anesthetized by intraperitoneal injection of urethane (50 μl of 10 % solution per 10 g body weight) and chlorprothixene (100 μl of 0.5 % solution per 10 g body weight). For the device sewing in the biological tissue, we used the tungsten microneedle with the diameter of 50 μm, which was manipulated by hand with tweezers. By guiding the tungsten needle, the fabricated thread-bioprobe was punched and embedded into the medial gastrocnemius (MG) muscle. Fig. 2b depicts two of the three Pt black microelectrodes that were placed on the muscle surface while the other one was embedded in the muscle. For multichannel recording, three microelectrodes were embedded in the muscle (picture not depicted). During the recording, the nerve corresponding to the MG muscles was electrically stimulated with a current ranging from +0.1 to +1.0 mA, 0.1 mA step, with a 100 μs duration at 1 s intervals (100 trials for each current range). No response was observed from these three microelectrodes to the stimuli ranging from +0.1 to +0.2 mA (Fig. 2c1). However, a response could be observed at the current stimulation of +0.3 mA; further, a response clearly appeared at the current stimuli of more than +0.5 mA (Fig. 2c2). Because the latency of responses is approximately 5 ms, the waveforms that were recorded via the three microelectrodes were considered to be the electromyography (EMG) signals that were generated by the current stimuli to the nerve.

We further investigated the device displacement through the cycling tests of the muscle stimulation. Fig. 2d shows a set of photographs before and after the stimulation for 500 trials. Herein, two of the three microelectrodes (Pt black) were placed on the muscle surface for the displacement observation, while the other one (upper right in each picture) was embedded in the muscle. The device displacement analysis was performed by measuring the distance between positions of an electrode and a blood vessel as shown in the photograph. After 500 trials, this distance was measured as approximately 3 μm.

The multichannel neuronal signal recording within the tissue for both acute and chronic cases can be obtained by applying the designed parylene-thread bioprobe; however, the tissue damage associated with the device penetration via the tungsten needle by hand (as earlier demonstrated using muscle, Fig. 2) should be minimized. To overcome the issue of tissue damage, a surgical sewing method of using a dissolvable material of polyethylene glycol (PEG) is proposed. Because PEG shows both the liquid and solid phases at varying temperatures (~60 °C), it enables the 'catch' and 'release' of the tungsten needle during manipulation without significant needle displacement (< 50 μm), as explored in the penetration using a gelatin brock (Fig. S4).

Fig. 3a shows the proposed surgical procedure in the sewing of parylene-thread bioprobe into the mouse brain tissue. The tungsten microneedle, which was held by a manipulator (first manipulator) via PEG, penetrated the tissue and passed through the two holes of cranial opening (Fig. 3a-1). The tip portion of the tungsten needle was subsequently caught using a liquid–PEG of the other manipulator (second

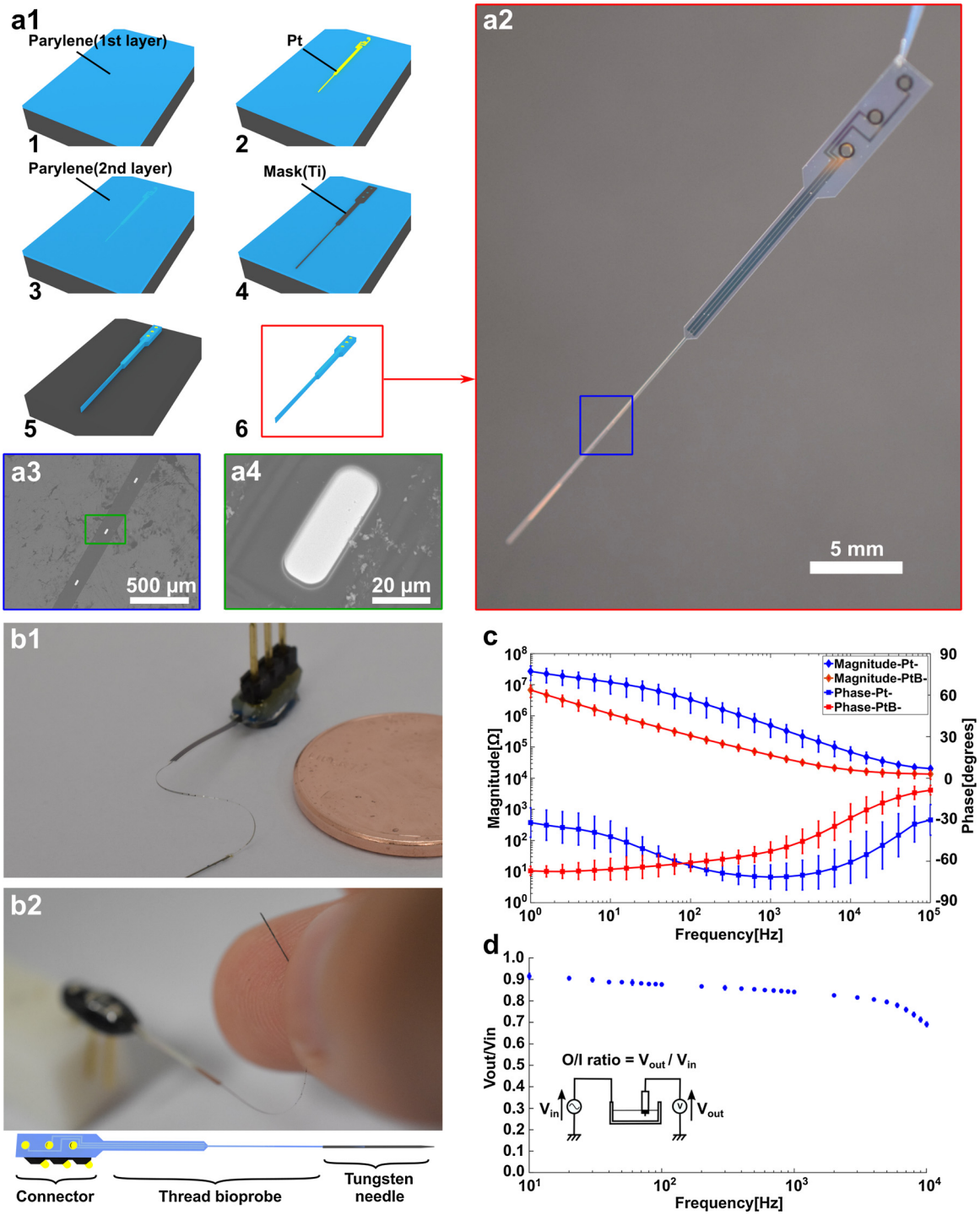

Fig. 1. A sewing flexible parylene-thread bioprobe device. a1) Device fabrication process steps: (1) first, parylene deposition on a substrate (Si); (2) Pt layer as both the electrode-site and the device interconnection that was formed on parylene by sputtering and etching; (3) second parylene deposition; (4, 5) parylene patterning by O_2 plasma with a Ti-mask; and (6) release of parylene film from the substrate using ethanol. a2) Photograph of overview of the device. a3, a4) Insets of blue and green squares that denote the SEM images of an array of three Pt microelectrodes and one electrode in the device, respectively. Each electrode's size is 10 μm × 40 μm. The overall length of the device is 33,000 μm. The needle portion with the length of 15,000 μm has an array of three Pt microelectrodes (10 μm × 40 μm) with a spacing of 500 μm (Fig. S1). b1, b2) Photographs showing the packaging device. The tip portion of the bioprobe is connected to a tungsten microneedle; further, each electrode's pad at the other device-side is connected to conventional pin connectors (three channels). c) The impedance characteristics of Pt black plated microelectrodes measured in phosphate buffered saline (PBS) at room temperature. d) Output/input signal amplitude ratios of Pt black microelectrodes measured in PBS. Test signals of 300 μV peak-to-peak sinusoidal waves from 1 Hz to 10,000 Hz are applied to the PBS. (For interpretation of the references to colour in the Figure, the reader is referred to the web version of this article).

manipulator, Fig. 3a-2), which was cooled and solidified for holding of the needle. By dropping solution (PBS) on the PEG at the first manipulator, the tungsten needle was released from the manipulator; however, the needle was held by the second manipulator (Fig. 3a-3). The tungsten needle was continuously pulled using the second manipulator, resulting in a flexible thread-bioporobe device and that was

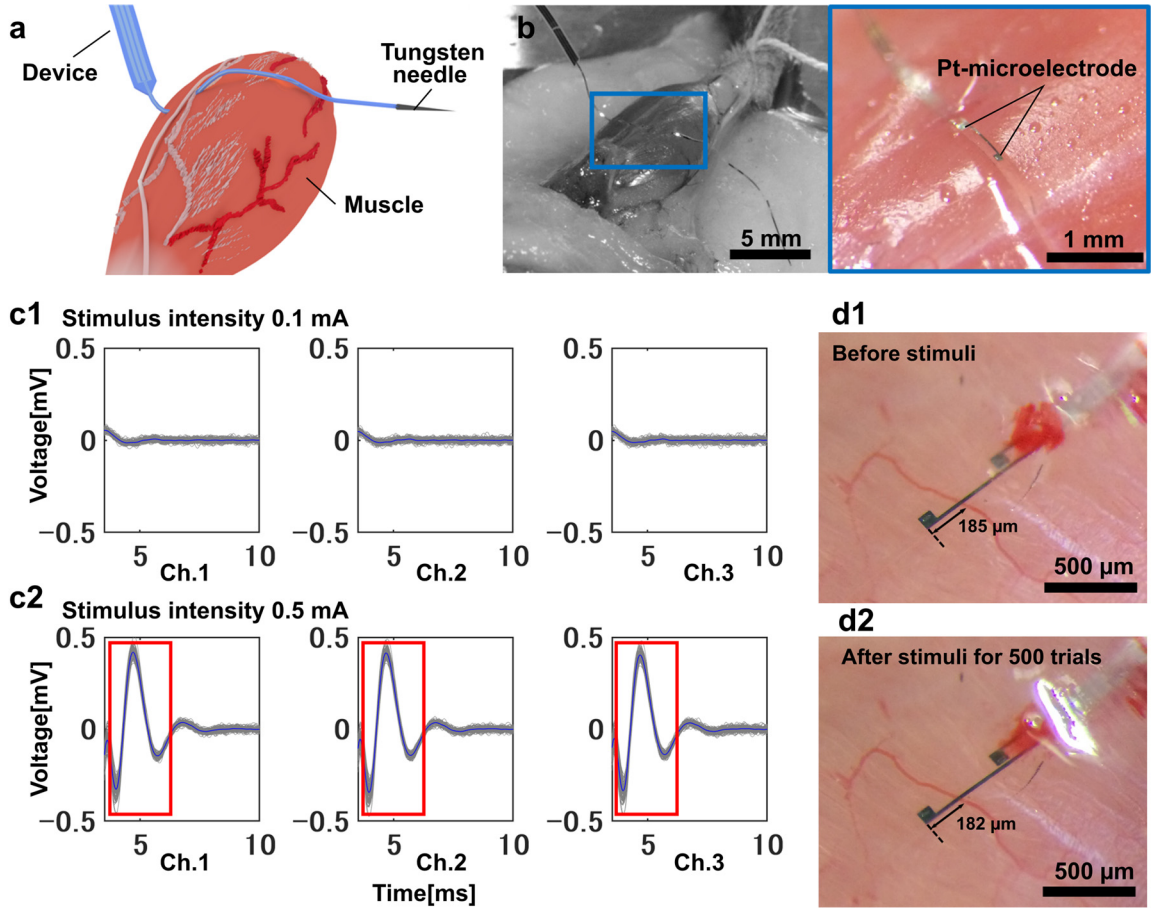

Fig. 2. The sewing and signal recording capabilities of the fabricated flexible thread-bioprobe device, demonstrated using the muscle of a mouse's leg *in vivo*. a, b) Schematic of the device, which was sewn to the MG muscle in the mouse's leg by guiding the tungsten microneedle. c1, c2) Signal waveforms recorded from the muscle via three Pt black microelectrodes embedded in the muscle, during the electrical stimuli to the corresponding nerve: 0.1 mA (c1) and 0.5 mA (c2). d) Device displacement during the muscle stimuli for 500 trials. The device displacement was analyzed by measuring the distance between the microelectrode and the blood vessel in each photograph (before and after).

placed inside the mouse's brain tissue (Fig. 3a-4). As a surgical advantage, the positions of microelectrodes in the tissue can be monitored precisely by the second manipulator.

Fig. 3b depicts the cranial opening area in which the thread-bioprobe device penetrated the brain tissue. Herein, the cranial opening area measured 1–3 mm in diameter, and the device's footprint in the tissue was approximately 150 μm in diameter (the diameter of the tungsten needle is 50 μm; the width and thickness of the parylene device are 150 and 10 μm, respectively). Using this surgical procedure, the tissue damage can be minimized, as confirmed by the minor bleeding in the tissue after the trials for more than five times.

The *in vivo* acute neuronal recording capability was also demonstrated using the mouse's brain (Fig. 4a). The mouse (male, 20–25 g) was anesthetized by intraperitoneal injection of urethane (50 μl of 10 % solution per 10 g body weight) and chlorprothixene (100 μl of 0.5 % solution per 10 g body weight). To record the visual response, after the cranial opening (3.2–3.5 mm on the lateral side and 4.0 mm on the caudal side from the bregma, having a diameter of 1–3 mm), the fabricated thread-bioprobe consisting of Pt-black plated three microelectrodes was inserted into the tissue and placed in the cortical layers of the primary visual cortex (V1) on the right hemisphere (~ 2.5 mm on the lateral side and 4.0 mm on the caudal side from the bregma) by manipulating the tungsten microneedle (50 μm diameter) with PEG (Fig. 4b). With the needle's guide, each microelectrode (Pt black, 10 μm × 40 μm in area) was precisely positioned in the tissue achieving lateral distances of 3.0 mm for Ch. 1, 2.5 mm for Ch. 2, and 2.0 mm for Ch. 3 along with the device penetration (Fig. 4b). As a visual stimulus, a light emitting diode (LED) array, consisting of nine white LEDs on a 20-mm wide substrate, was used.

While visual stimuli was applied to the mouse's eye for 0.5 s, neuronal responses were repeatedly recorded via the three embedded microelectrodes in the tissue (Fig. 4c). The second panel in Fig. 4c represents low frequency-band (filtering = 10–500 Hz), whereas third panel shows high frequency-band (filtering = 500–3000 Hz) waveforms recorded by each microelectrode. The low frequency-band waveform signals appeared at around 0.25 s, which were consistent with the latency of the visual response, were subjected to be the LFP evoked by the visual stimuli. Bottom two panels show raster plots and peristimulus time histograms (PSTHs), respectively, taken from each high frequency-band signals. The detection thresholds for each channel was 4 times the standard deviation (σ) of the mean signal – 0.5 to −1.0 s before the stimulus onset. However, no significant responses to the visual stimulus were obtained. This was probably due to the creation of a gap between the recording electrodes and their neuronal signal sources [1–3,23] (the geometries of our device are 50 μm diameter for tungsten needle, 150 μm width for parylene-thread, and 150 μm width for the resin junction, Fig. S2).

The chronic *in vivo* neuronal recording ability was also demonstrated using the mouse's brain (Fig. 5a). The mouse (male, 20–25 g) was anesthetized by isoflurane, and Pt black plated three microelectrodes were inserted into the mouse brain tissue using the surgical procedure similar to the acute recording (Fig. 4a). Using dental resin (Fig. 5a), the thread-bioprobe and pin-connector were attached to the cranium. Here, a gelatin sponge was placed around the thread-bioprobe

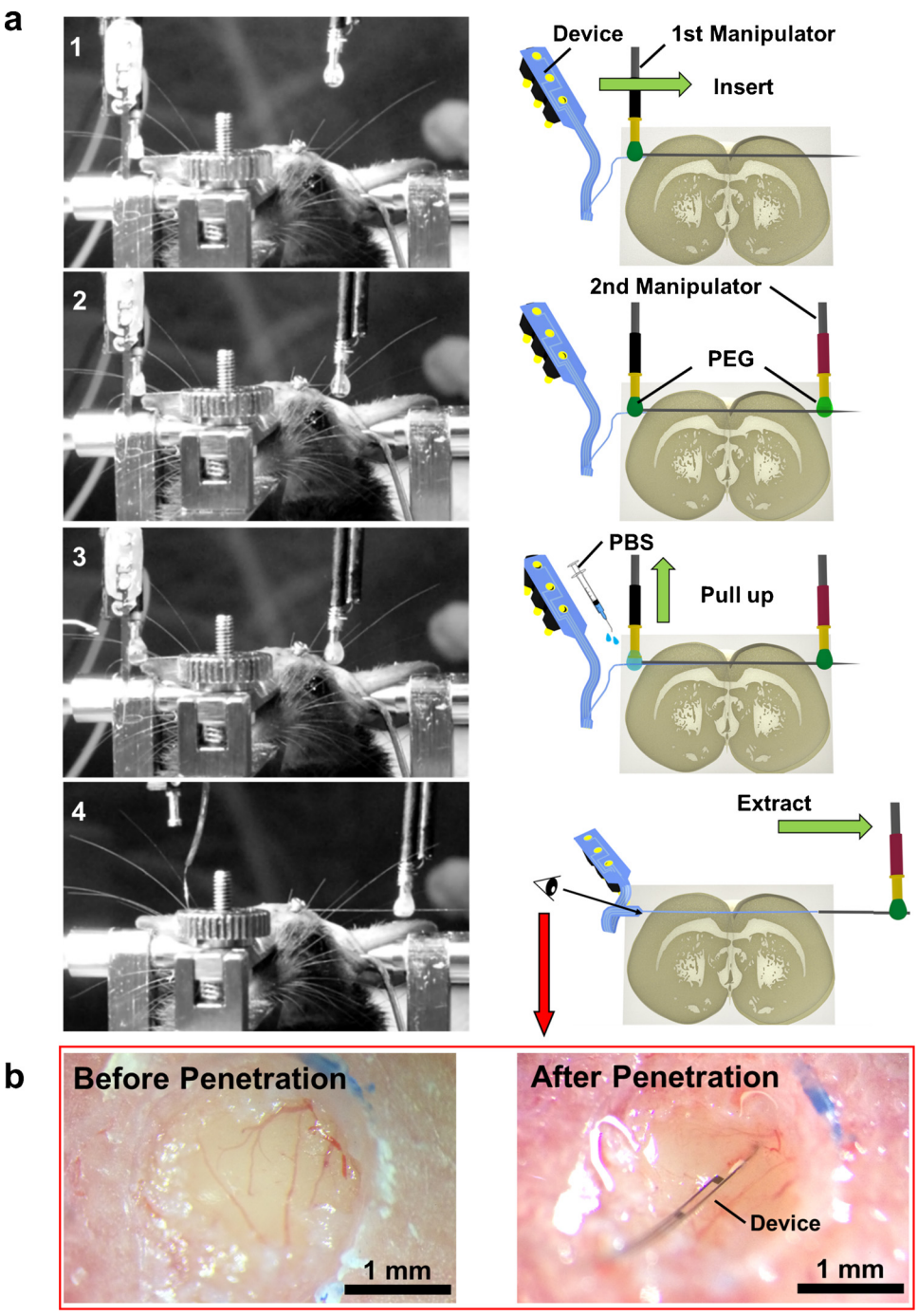

Fig. 3. A proposed surgical procedure with a dissolvable material of PEG for the brain tissue of mice. a) Schematic of each step in the surgical procedure: (1) tungsten microneedle penetrates through the tissue while the needle is held with PEG at first manipulator; (2) the tip portion of the tungsten needle that is caught using the second manipulator with PEG; (3) release of the tungsten needle from the first manipulator by dipping PBS to the PEG; and (4) continuous pulling of the tungsten needle with the second manipulator for placing the flexible thread-bioprobe device within the tissue. b) Photographs depicting the cranial opening area of the brain tissue before and after device penetration.

to protect the brain surface from infection. An array of LEDs was used to record the visual responses as used in the acute recording (Fig. 4).

Signals from the free moving mouse were recorded a week after the thread-bioprobe implantation (Fig. 5b). Visual stimuli were applied to the mouse's eye for 0.5 s, and the responses were continuously recorded by the three microelectrodes. The second and third panels in Fig. 5b represent low frequency-band (filtering = 10–500 Hz) and high frequency-band (filtering = 500–3000 Hz) waveforms recorded by each microelectrode, respectively. The two panels at the bottom show raster plots and histograms, respectively, obtained from each high frequency-band signals (the detection threshold of each channel was 4σ of the mean signal – 0.5 to −1.0 s before the stimulus onset). These waveform signals, which appeared at around 0.25 s were consistent with the latency of the visual response, were subjected to be the LFPs (second panels in Fig. 5b) and spikes (third panels in Fig. 5b) evoked by the visual stimuli.

In order to observe the influence of the surgical procedure of sewing on the mouse, the change in the mouse's body weight was continuously monitored for two weeks (Fig. 5c). Initially, we observed decrease in mouse's weight for three consecutive days after surgery and a recovery on the seventh day. This suggested that the proposed surgical method of sewing of the fabricated parylene-thread-bioprobe was applicable to the chronic recording on the mouse.

4. Discussion

The parylene–based flexible thread-bioprobe device was designed and fabricated. The tip portion of the device was connected to the tungsten microneedle with a UV-curable resin, enabling the device penetration into the tissue. The resin formed between the tip of

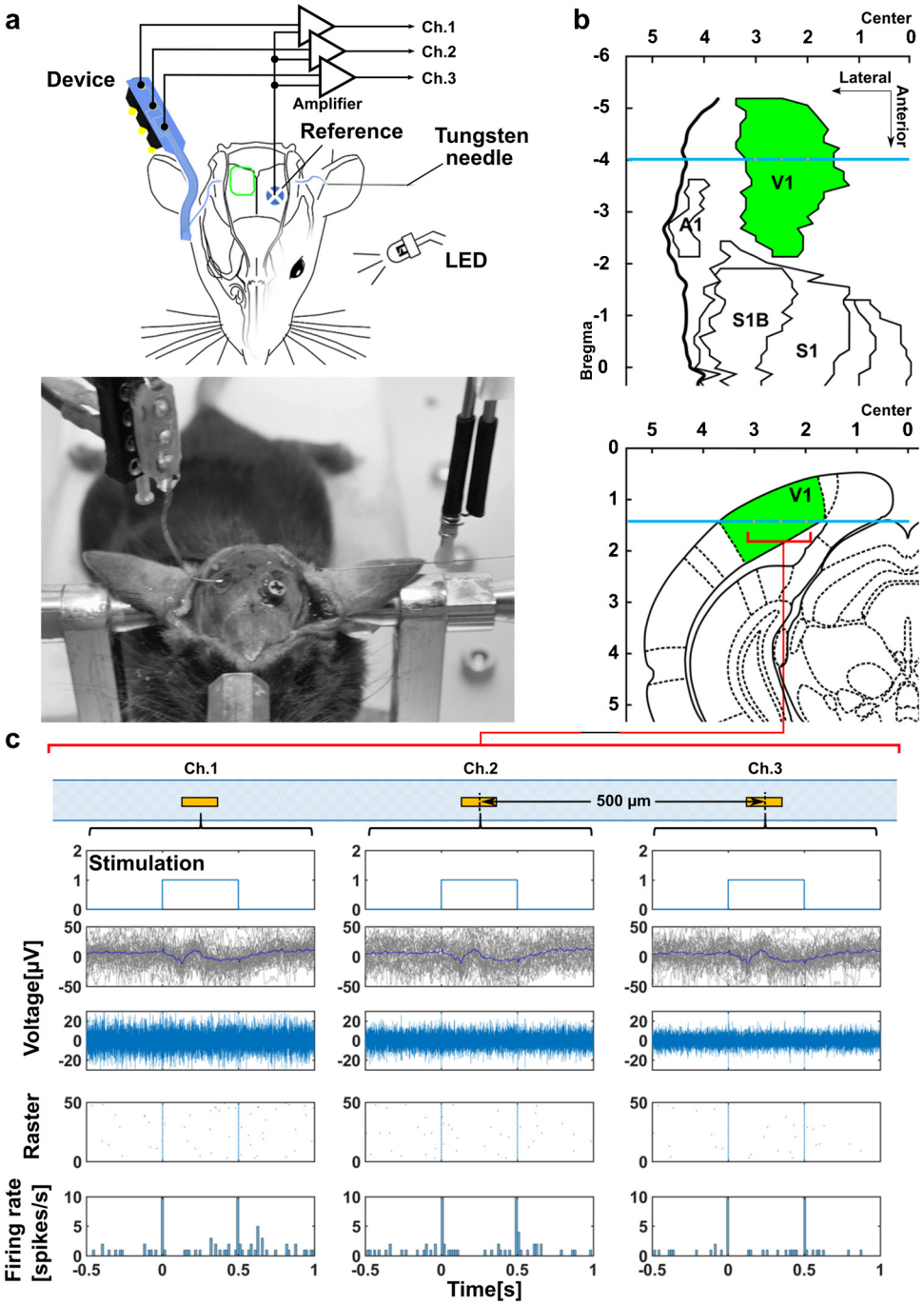

Fig. 4. Acute *in vivo* neuronal recording using mouse brain. a) Schematic of the recording setup and photograph of the bioprobe device sewn to the brain tissue by guiding the tungsten microneedle with PEG. An LED array was used for visual stimulation. b) Tangential and coronal schematics of the primary visual cortex (V1) based on stereotaxic coordinate, illustrating the position of the thread-bioprobe in the tissue. Blue lines and yellow dots in both schematics represent the footprint of thread-bioprobe and microelectrodes (Pt black), respectively. c) Signal waveforms recorded from the V1 via three embedded microelectrodes in the tissue. Top panels represent timing of the optical stimulation. Second and third panels are low-frequency-band (filtering = 10–500 Hz, n = 50 trials) and high frequency-band (filtering = 500–3000 Hz, single trial) signal waveforms, respectively. Bottom two panels are raster plots and PSTHs, respectively, taken from the high frequency signals (n = 50 trials). The detection thresholds for each channel was 4 times the standard deviation σ of the mean signal − 0.5 to −1.0 s before the stimulus onset. (For interpretation of the references to colour in the Figure, the reader is referred to the web version of this article).

parylene-thread and the root of tungsten needle, achieves a connection geometry of < 150 μm in width (Fig. S2). As demonstrated in both the recordings using mouse's brain tissue as well as limb muscle, these tissues could be punched with a flexible thread-bioprobe following the guidance of the tungsten microneedle. During the tissue penetration, no separation of the tungsten needle from the parylene-thread was observed, indicating that the junction of UV-curable resin is strong enough to sustain tissue punching.

The penetrating and recording capabilities of the fabricated parylene–based flexible device were confirmed on the limb muscle of the mouse. During the electrical stimulation, the limb showed large displacement associated with the relaxation and contraction. However, as confirmed from the recording sessions for 500 trials, no significant electrode displacements (< 5 μm, Fig. 2d) could be observed because the thread-device was sewn to the muscle. The advantage of being able to sew microelectrodes with the tissue can be applied to other organs and tissues that exhibit large displacement and deformation (e.g., pulsation). As to the position of microelectrodes within the muscle, because of the diameter of the guiding tungsten needle (50 μm diameter), it was assumed that the thread-bioprobe penetrated the tissue between fascicles (a group of muscle cells) in the skeletal muscle (groups of fascicles). Compared to the device placement over the surface of the skeletal muscles, such an electrode positioning within the skeletal muscles enables us to detect signals inside the muscle, offering advantages for further analysis in muscles (e.g., three-dimensional signal mapping of the muscle).

In terms of physical effects on the brain tissue, the device features of small geometry and flexibility offer various advantages, including less destabilization of intracranial pressure, reduction of the infection risk, and less amount of damage of the brain tissue and blood vessels located

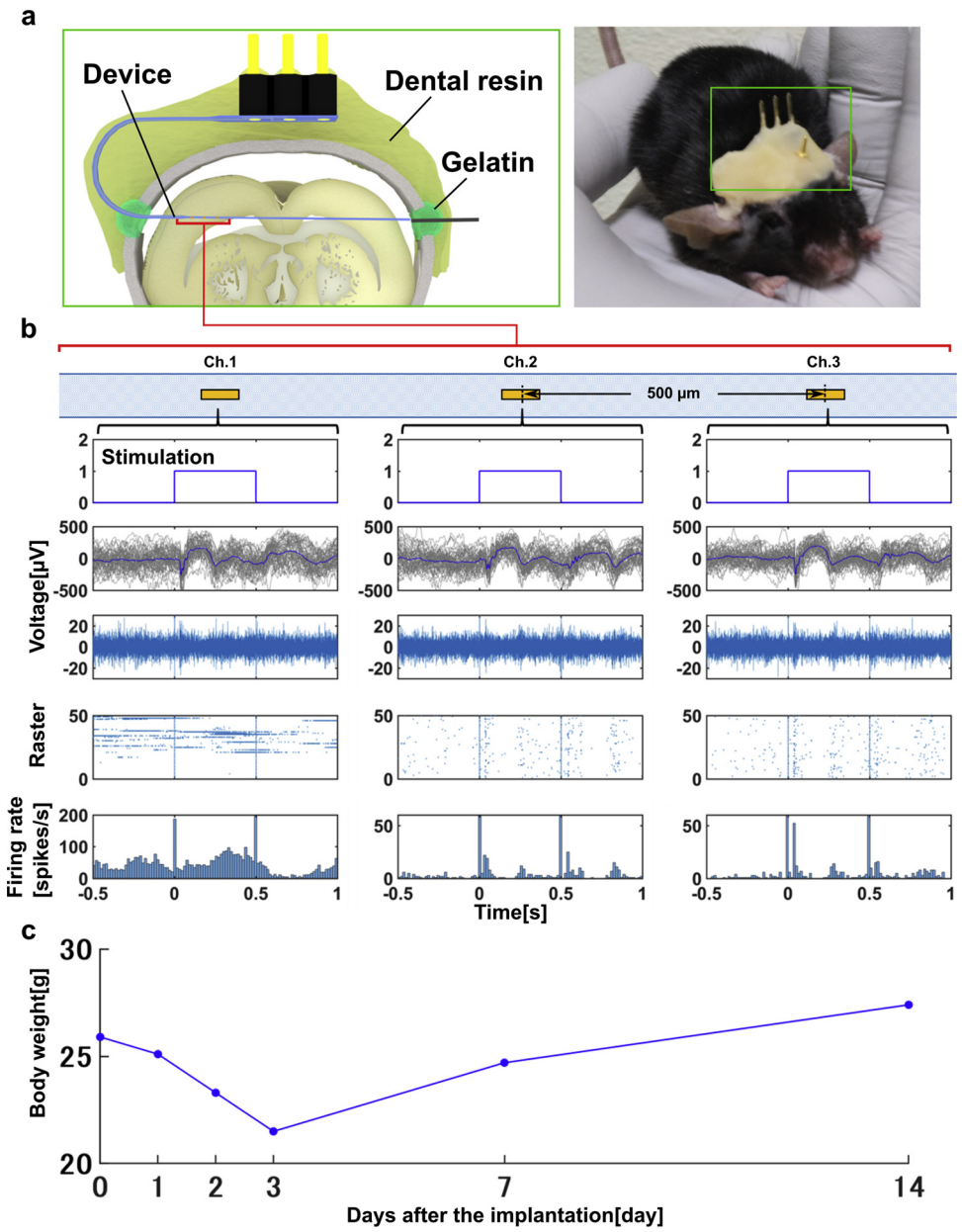

Fig. 5. Chronic *in vivo* neuronal recording using mouse brain. a) Schematic of the surgical procedure for the chronic recording and the photograph of the mouse that was implanted thread-bioprobe. The parylene-thread bioprobe device was implanted in the visual cortex (V1) in the right hemisphere of the mouse. For the recording of the visual responses from the mouse, we used an array of white LEDs. b) Waveforms recorded from the free moving mouse a week after the implantation via three microelectrodes in the V1. Top panels represent timing of the optical stimulation. Second and third panels are low-frequency-band (filtering = 10–500 Hz, n = 50 trials) and high frequency-band (filtering = 500–3000 Hz, single trial) signal waveforms, respectively. Bottom two panels are raster plots and PSTHs, respectively, taken from the high frequency signals (n = 50 trials). The detection thresholds for each channel was 4 times the standard deviation σ of the mean signal − 0.5 to −1.0 s before the stimulus onset. c) Mouse's weight depending on the day after the implantation of thread-device.

beneath the bone. Theoretically, the required opening area of craniotomy is considered to be adequate with the cross-sectional areas for both the tungsten needle (50 μm diameter) and the parylene-thread device (150-μm wide and 10-μm thick). In addition, because the tungsten microneedle exhibited sufficient hardness, it was not necessary to remove the dura matter, reducing the risk of infection during long-period recordings.

The advantages of the proposed surgical procedure of sewing with PEG include the reduction of the physical influence on the tissue and the risk of infection as well as precise position control of the flexible microelectrode in the tissue. Since the "catch" and "release" of tungsten microneedle was done in dissolvable PEG, its displacement of the tungsten-needle during the sewing ranged within 50 μm (Fig. S4), greatly reduced compared to conventional ways with undesirable physical stress on the needle. While recording the brain tissue, precise placement of microelectrodes is considered to be important for determining the recording region. As demonstrated in case of device penetration using a mouse brain tissue, both the direction and the distance of the tungsten needle's penetration were determined by referring to the bregma and the lambda, while the position of three microelectrodes (500 μm apart) in the tissue were determined by manipulating the tungsten needle (Fig. 4b). For performing acute recording, the position of the thread-bioprobe as well as microelectrodes in the tissue could be fixed by the manipulator system after extracting the tungsten needle from the tissue. In the chronic recordings, each side of the thread-bioprobe's portion was fixed to the cranium with dental resin while the thread-bioprobe was passed through the two narrow openings (1–3 mm diameter) in the cranium at each side. This method enabled the fixation of the flexible device within the tissue with little or no significant misalignment or displacement during the implantation.

Based on the parylene-MEMS process, the geometry of the fabricated thread-bioprobe can further be reduced by decreasing both factors, such as sizes of the recording site (10 μm × 40 μm area) and the device interconnection (20-μm width) with reduced mask patterns. Since contact printing–based photolithography was used, these pattern sizes will be reduced through i) electron beam–based lithography and ii) multiple layers of device interconnection. It is also possible to combine both processes. These fabrication processes also enable the increase in the number of microelectrodes, permitting the application of the device in bio-signal recording applications.

5. Conclusion

In summary, the flexible parylene-thread bioprobe was fabricated, and the tissue was penetrated by guiding the tungsten microneedle based on the sewing mechanism. The fabricated thread-bioprobe enabled us to acquire EMG signals from a mouse's MG muscle and neuronal signals of LFP and spike from the mouse's visual cortex *in vivo*. The proposed thread-bioprobe device that exhibits the features of device flexibility, electrode position controllability, and implantation capability will contribute to both acute and chronic *in vivo* electrophysiological recordings. The sewing method of the flexible thread device using a dissolvable material of PEG has been proposed to prevent physical stress on the tissue. These features of both flexible thread-device and surgical method proved unachievable earlier using conventional methods and devices.

6. Experimental section

All experimental procedures using animals were approved by the committees for the use of animals at Toyohashi University of Technology, and all animal care followed the Standards Relation to the Care and Management of Experimental Animals (Notification No. 6, March 27, 1980 of the Prime Minister's Office of Japan)

Declaration of Competing Interest

The authors declare that they have no known competing financial interests or personal relationships that could have appeared to influence the work reported in this paper.

Acknowledgements

This work was supported by Grants-in-Aid for Scientific Research (B) (No. 17H03250), for Young Scientist (A) (No. 26709024), on Innovative Areas (Research in a proposed research area) (No. 15H05917), and Strategic Advancement of Multi-Purpose Ultra-Human Robot and Artificial Intelligence Technologies program from NEDO. R.N. was supported by Takeda Science Foundation. K.K. was supported by Toyota Physical & Chemical Research Institute Scholars.

Appendix A. Supplementary data

Supplementary material related to this article can be found, in the online version, at doi:https://doi.org/10.1016/j.snb.2020.127835.

References

[1] R. Biran, D.C. Martin, P.A. Tresco, Neuronal cell loss accompanies the brain tissue response to chronically implanted silicon microelectrode arrays, Exp. Neurol. 195 (2005) 115–126.
[2] V.S. Polikov, P.A. Tresco, W.M. Reichert, Response of brain tissue to chronically implanted neural electrodes, J. Neurosci. Methods 148 (2005) 1–18.
[3] H. Szarowski, D. Andersen, S. Retterer, J. Spence, M. Isaacson, G. Craighead, N. Turner, W. Shain, Brain responses to micro-machined silicon devices, Brain Res. 983 (2003) 23–35.
[4] Y. Zhong, R.V. Bellamkonda, Biomaterials for the central nervous system, J. R. Soc. Interface 5 (2008) 957–975.
[5] J.P. Seymour, D.R. Kipke, Neural probe design for reduced tissue encapsulation in CNS, Biomaterials. 28 (2007) 3594–3607.
[6] J.W. Jeong, G. Shin, S. Il Park, K.J. Yu, L. Xu, J.A. Rogers, Soft materials in neuroengineering for hard problems in neuroscience, Neuron. 86 (2015) 175–186.
[7] R.J. Vetter, J.C. Williams, J.F. Hetke, E.A. Nunamaker, S. Member, D.R. Kipke, Chronic neural recording using silicon-substrate microelectrode arrays implanted in cerebral cortex, IEEE Trans. Biomed. Eng. 51 (2004) 896–904.
[8] E.K. Purcell, D.E. Thompson, K.A. Ludwig, D.R. Kipke, Flavopiridol reduces the impedance of neural prostheses in vivo without affecting recording quality, J. Neurosci. Methods 183 (2009) 149–157.
[9] T. Kim, J.G. McCall, Y.H. Jung, X. Huang, E.R. Siuda, Y. Li, J. Song, Y.M. Song, H.A. Pao, R.-H. Kim, Injectable, cellular-scale optoelectronics with applications for wireless optogenetics, Science. 340 (2013) 211–216.
[10] H.S. Sohal, A. Jackson, R. Jackson, G.J. Clowry, K. Vassilevski, A. O'Neill, S.N. Baker, The sinusoidal probe: a new approach to improve electrode longevity, Front. Neuroeng. 7 (2014) 10.
[11] J. Liu, T.M. Fu, Z. Cheng, G. Hong, T. Zhou, L. Jin, M. Duvvuri, Z. Jiang, P. Kruskal, C. Xie, Z. Suo, Y. Fang, C.M. Lieber, Syringe-injectable electronics, Nat. Nanotechnol. 10 (2015) 629–635.
[12] L. Luan, X. Wei, Z. Zhao, J.J. Siegel, O. Potnis, C.A. Tuppen, S. Lin, S. Kazmi, R.A. Fowler, S. Holloway, A.K. Dunn, R.A. Chitwood, C. Xie, Ultraflexible nanoelectronic probes form reliable, glial scar–free neural integration, Sci. Adv. 3 (2017) 1–10.
[13] A. Lecomte, V. Castagnola, E. Descamps, L. Dahan, M.C. Blatché, T.M. Dinis, E. Leclerc, C. Egles, C. Bergaud, Silk and PEG as means to stiffen a parylene probe for insertion in the brain: toward a double time-scale tool for local drug delivery, J. Micromechanics Microengineering 25 (2015).
[14] S. Felix, K. Shah, D. George, V. Tolosa, A. Tooker, H. Sheth, T. Delima, S. Pannu, Removable silicon insertion stiffeners for neural probes using polyethylene glycol as a biodissolvable adhesive, Conf. Proc. IEEE Eng. Med. Biol. Soc. (2012) 871–874.
[15] L.W. Tien, F. Wu, M.D. Tang-Schomer, E. Yoon, F.G. Omenetto, D.L. Kaplan, Silk as a multifunctional biomaterial substrate for reduced glial scarring around brain-penetrating electrodes, Adv. Funct. Mater. 23 (2013) 3185–3193.
[16] S. Yamagiwa, M. Ishida, T. Kawano, Flexible parylene-film optical waveguide arrays, Appl. Phys. Lett. 107 (2015) 1–6.
[17] Y. Morikawa, S. Yamagiwa, H. Sawahata, R. Numano, K. Koida, M. Ishida, T. Kawano, Ultrastretchable kirigami bioprobes, Adv. Healthc. Mater. 7 (2018) 1701100.
[18] S. Yamagiwa, M. Ishida, T. Kawano, Self-curling and-sticking flexible substrate for ECoG electrode array, in: micro electro mechanical systems (MEMS), 2013, IEEE 26th International Conference On, IEEE (2013) 480–483.
[19] H. Oka, K. Shimono, R. Ogawa, H. Sugihara, M. Taketani, A new planar multielectrode array for extracellular recording : application to hippocampal acute slice, J. Neurosci. Methods 93 (1999) 61–67.
[20] A. Fujishiro, H. Kaneko, T. Kawashima, M. Ishida, T. Kawano, In vivo neuronal action potential recordings via three-dimensional microscale needle-electrode arrays, Sci. Rep. 4 (2014) 4868.
[21] H. Sawahata, S. Yamagiwa, A. Moriya, T. Dong, H. Oi, Y. Ando, R. Numano, M. Ishida, K. Koida, T. Kawano, Single 5 μm diameter needle electrode block modules for unit recordings in vivo, Sci. Rep. 6 (2016) 35806.
[22] T. Harimoto, K. Takei, T. Kawano, A. Ishihara, T. Kawashima, H. Kaneko, M. Ishida, S. Usui, Enlarged gold-tipped silicon microprobe arrays and signal compensation for multi-site electroretinogram recordings in the isolated carp retina, Biosens. Bioelectron. 26 (2011) 2368–2375.
[23] D.J. Edell, V. Van Toi, V.M. Mcneil, L.D. Clark, Factors influencing the biocompatibility of insertable silicon microshafts in cerebral cortex, IEEE Trans. Biomed. Eng. 39 (1992) 635–643.

Koji Yamashita completed his B.S. degree in 2017 and M.S. degree in 2019 from the Department of Electrical and Electronic Engineering, Toyohashi University of Technology, Japan. He is pursuing his Ph.D. from the Department of Electrical and Electronic Engineering, Toyohashi University of Technology, Japan.

Hirohito Sawahata had been a Postdoctoral Research Fellow during 2009–2012 at Graduate school of Medical and Dental sciences, Niigata University, Japan and completed his Ph.D. from Graduate School of Science and Engineering, Yamagata University, Japan. During 2012–2013 he worked as an Assistant Professor at Graduate School of Medical and Dental sciences, Niigata University, Japan. During 2013–2017, he is working as an Assistant Professor, Department of Electrical and Electronic Information Engineering, Toyohashi University of Technology, Japan. During 2017–2018, he was a Postdoctoral Research Fellow, National Institute of Advanced Industrial Science and Technology (AIST), Japan. From 2019, he was as an Assistant Professor, National Institute of Technology (KOSEN), Ibaraki College, Japan.

Shota Yamagiwa completed his M.S. degree in 2012, Ph.D. degree in 2016, and between 2004 and 2005, he was a Postdoctoral Research Fellow at Department of Electrical and Electronic Engineering, Toyohashi University of Technology, Japan. He is working as a Postdoctoral Research Fellow, Department of Electrical and Electronic Information Engineering, Toyohashi University of Technology, Japan.

Yusuke Morikawa completed his B.S. degree in 2015 and M.S. degree in 2017 from the Department of Electrical and Electronic Engineering, Toyohashi University of Technology, Japan. In 2018, he was a visiting student in the Department of Microsystems Engineering at the University of Freiburg, Germany. He is pursuing his Ph.D. from the Department of Electrical and Electronic Engineering, Toyohashi University of Technology, Japan.

Rika Numano completed her B.Sc. in 1996, M.Sc. in 1998, and Ph.D. in 2002, all from Faculty of Technology, University of Tokyo, Japan. She was a Postdoctoral Research Fellow (Japan Society for the Promotion of Science), Human Genome Center Institute of Medical Science, University of Tokyo, Japan between 2002 and2005, Postdoctoral Fellow (Japan Society for the Promotion of Science Postdoctoral fellowship for research abroad), Department of Molecular and Cell Biology, University of California Berkeley between 2005 and 2006, a researcher, Cell Function Dynamics, RIKEN between 2006 and 2007, a Researcher, ERATO Project, Japan Science and Technology Agency between 2007 and 2009 and Tenure-truck Associate professor, Electronics-Inspired Interdisciplinary Research Institute (EIIRIS),Toyohashi University of Technology, between 2009 and 2013. Currently, from 2013, she is working as an Associate professor, at Department of

Environmental and Life Sciences, Toyohashi University of Technology, Japan.

Kowa Koida completed his Ph.D. degree, Interdisciplinary Graduate School of Science and Engineering, Tokyo Institute of Technology, Japan in 2000. He had been a Postdoctoral Research Fellow during 2000–2007 at National Institute for Physiological Sciences, Japan. During 2007–2010 he worked as an Assistant Professor at the same institution. He is working as an Associate professor, Department of Computer and Science and Engineering, Toyohashi University of Technology, Japan, and Electronics Inspired-Interdisciplinary Research Institute (EIIRIS) at the same University.

Takeshi Kawano completed his M.S. degree in 2001, Ph.D. degree in 2004, and between 2004 and 2005, he was a Postdoctoral Research Fellow at Department of Electrical and Electronic Engineering, Toyohashi University of Technology, Japan. During 2005–2007, he was a Postdoctoral Research Fellow (Japan Society for the Promotion of Science Postdoctoral fellowship for research abroad), Department of Mechanical Engineering, Berkeley Sensor and Actuator Center (BSAC), University of California Berkeley. During 2007–2010 was an Assistant Professor, Toyohashi University of Technology, Electrical and Electronic Engineering, Japan. From 2010 on wards he has been PRESTO Researcher, Japan Science and Technology Agency (JST) as well as an Associate Professor, Electrical and Electronic Information Engineering Toyohashi University of Technology, Japan.